Vol 16 No 2, February 2007
1009-1963/2007/16(02)/0382-10

Chinese Physics

© 2007 Chin. Phys. Soc.
and IOP Publishing Ltd

Saturation effects on Ba 6pnl ($l = 0, 2$) and 6pnk ($|M| = 0, 1$) autoionization spectra*

Li Shi-Ben(李士本)[a)†] and Dai Chang-Jian(戴长建)[b)]

[a)] *Department of Physics, Wenzhou University, Wenzhou* 325027, *China*

[b)] *College of Science, Tianjin University of Technology, Tianjin* 300191, *China*

(Received 11 March 2006; revised manuscript received 31 August 2006)

Using a three-step laser saturation excitation technique, the saturation effects on the Ba 6pns ($J = 1$) and 6pnd ($J = 1$, 3) autoionization spectra are observed systemically in zero field. These saturation spectra are introduced to determine the high n members of 6pnl ($l = 0$, 2) autoionizing series and are used to analyse the channel interactions among the autoionizing series in zero field. Furthermore, the saturation excitation technique is applied to the electric field case, in which the saturation spectra of Ba 6pnk ($|M| = 0$, 1) autoionizing Stark states are measured. Most of these saturation spectra are observed for the first time so far as we know, which indicate the mixing of the autoionizing states in the electric fields.

Keywords: saturation excitation, isolated-core excitation, autoionizing state, electric field effect
PACC: 3260, 3280

1. Introduction

The saturation effect on the atomic autoionization spectrum, i.e. autoionization saturation spectrum, is an important approach to understanding the properties of autoionizing states in zero and electric fields. Over two decades, measurements on the autoionization saturation spectra of two-electron atoms, such as Mg, Ca, Sr and Ba atoms, have been extensively preformed in zero field by use of three-step laser saturation excitation method.[1−5] As an efficient spectroscopic technique, the three-step saturation excitation technique is similar to the three-step isolated-core excitation (ICE).[6,7] In the process of three-step laser saturation excitation, one of the valence electrons is excited to a Rydberg state in the first two steps, while the remaining core electron is placed in an excited state in the third step. Unlike the ICE in which the Rydberg electron nearly remains a spectator in the third step of excitation, 'shake-up' of the Rydberg electron cannot be ignored any more in the process of saturation excitation. The drastic shake-up of Rydberg electron leads to the obvious appearance of a series of satellitic peaks in the main profile of the autoionization spectrum. Therefore, the saturation spectrum provides more information about the autoionizing series than the ICE spectrum, which plays an important role in studying the correlation between the core and Rydberg electrons and thereby understanding the basic three-body Coulomb problem.[8]

It is not surprising that with the three-step laser saturation excitation, several researches on Ba 6pns ($J = 1$) and 6pnd ($J = 1, 3$) autoionization saturation spectra have been reported in zero field.[9−11] In these studies, one of the valence electrons is excited from the ground state to the ns or nd Rydberg state in the first two steps of transition, while the other valance electron is driven to the 6p state by the third laser. These studies mostly concentrate on the analysis of channel interaction between 6pns ($J = 1$) and 6pnd ($J = 1$, 3) autoionizing series. However, another application of the saturation spectra, the determination of high n members of the autoionizing series, is always neglected. Because the high n state has a comparatively small cross section, it is very difficult to excite this state in the ICE process, even with the help of the high-resolution laser.[12] Therefore, it is still necessary to study systemically the saturation spectra of Ba 6pns ($J = 1$) and 6pnd ($J = 1$, 3) autoionizing states in zero field.

Since all real environments include the electric field naturally, it is logical to extend the spectrum

*Project supported by the National Natural Science Foundation of China (Grant No 10574098), the Natural Science Foundation (Grant No 05YFJMJC05200) of Tianjin, and the Scientific Research Fund of Zhejiang Provincial Education Department.
†E-mail: shibenli@wzu.edu.cn

study of autoionizing states to the case of electric field. The autoionization spectrum in electric field, namely the autoionization Stark spectrum, may reveal the effects of electric fields on the autoionizing states, such as the mixing of the autoionizing states in electric fields. Many contributions have been devoted to the properties of the autoionizing Stark states. For example, Jones and Gallagher measured a series of Ba $6p_{1/2}nk$ ($|M| = 0$) autoionization spectra in electric fields, in which the autoionization rates of these autoionizing Stark states have been measured and discussed.[13] Recently, our group reported the Ba 6pnk ($n = 13 - 15$, $|M| = 1$) autoionization Stark spectra measured using the ICE method for the first time, clearly exhibiting that the autoionization rates of these states depend on the strength of static electric field.[14,15] Certainly, compared with the ICE Stark spectra, the saturation effects on their Stark spectra can provide more information about the mixing mechanism in the presence of electric fields. However, few references have reported the saturation spectra of Ba 6pnk ($n = 13$, $|M| = 0$) autoionizing states in electric fields,[16] while the study on the Ba 6pnk ($|M| = 1$) autoionizing saturation spectra still remains untouched.

In this paper, the three-step laser saturation excitation technique is employed to measure systemically the saturation spectra of Ba 6pns ($J = 1$) and 6pnd ($J = 1$, 3) autoionizing states in zero field, in which the saturation spectra are used to determine the high n members of the 6pns ($J = 1$) and 6pnd ($J = 1$, 3) autoionizing series and discuss the channel interaction between these autoionizing series in zero field. Furthermore, with this method the saturation effects on the 6pnk ($n = 13 - 15$, $|M| = 0$, 1) autoionization spectra are also observed for the different strengths of electric fields. These newly observed autoionization Stark spectra display the mixing process of autoionizing states in the presence of electric fields.

The rest of this paper is organized as follows: first, we briefly describe the experimental method for measuring autoionization saturation spectra in Section 2, and then outline the theoretical basis about the autoionization saturation spectra in Section 3. Then the experimental results will be interpreted and discussed in detail in Section 4. Finally, main conclusions will be drawn in Section 5.

2. Experimental method

Since the experimental setup is similar to those used in our previous works, here we only briefly describe the main features relevant to the present experiment.[12,14] Three dye lasers are pumped by a pulsed Nd:YAG laser, which runs at a 10-Hz repetition rate. The laser polarization direction is controlled by a combination of rhomb and polarizer.[14] Three collinear laser beams reach the interaction region step by step so that the unnecessary excitation can be avoided. The Ba atom beam is produced from a resistively heated oven, which is crossed perpendicularly by the laser beam inside a vacuum chamber. With the three-step laser excitation, Ba atoms are excited to the 6pns or 6pnd autoionizing state in zero field and the 6pnk autoionizing states in electric fields. In particular, when the third laser wavelength is scanned across the 6s$\rightarrow$ $6p_{1/2}$ or 6s$\rightarrow$ $6p_{3/2}$ resonance line, the autoionizing states with the corresponding $6p_{1/2}$ or $6p_{3/2}$ core can be obtained in zero and electric fields. The Ba atoms in autoionizing states decay quickly into electrons and ions. The ion signals that represent the autoionization spectra are collected by applying a pulsed electric field so as to be detected by a microchannel plate (MCP) detector, and then input into a boxcar integrator. Finally, the autoionization spectra are recorded and stored in a computer for further analysis.

Similar to the three-step ICE method, the three-step saturation excitation technique involves several energy levels in each step of excitation, as demonstrated in Fig.1. Two excitation cases, i.e. the zero field and the electric field cases, should be taken into account. In the zero field case, as shown in Fig.1(a), three lasers are all linearly polarized to the same direction of collection electric field. With this polarization combination only the transition with $\Delta m_J = 0$ and $|\Delta J| = 1$ is allowed. Under this restriction, the final state of the transition is the 6pns ($J = 1$) or 6pnd ($J = 1$, 3) autoionizing state, through the intermediate 6sns $^1S_0$ or 6snd $^{1,3}D_2$ Rydberg state, respectively. In the electric field case, all the excitation processes are in the presence of dc electric fields, which are parallel to the collection electric field. Two types of laser polarization combinations are used in this case, as shown in Fig.1(b). For the first type, the first two lasers are linearly polarized, parallel to the direction of the collection and dc electric fields, through the intermediate 6snk ($|M| = 0$) Stark states. This

type of polarization combination results in the 6pnk ($|M| = 0$) autoionizing Stark states. For the second type of polarization combination, the first two lasers are polarized at a right angle and lead to $\Delta m_J = \pm 1$ transitions, so that the 6snk ($|M| = 1$) Stark states can be excited. The third laser is scanned to excite the Ba atoms to the 6pnk ($|M| = 1$) autoionizing Stark states.

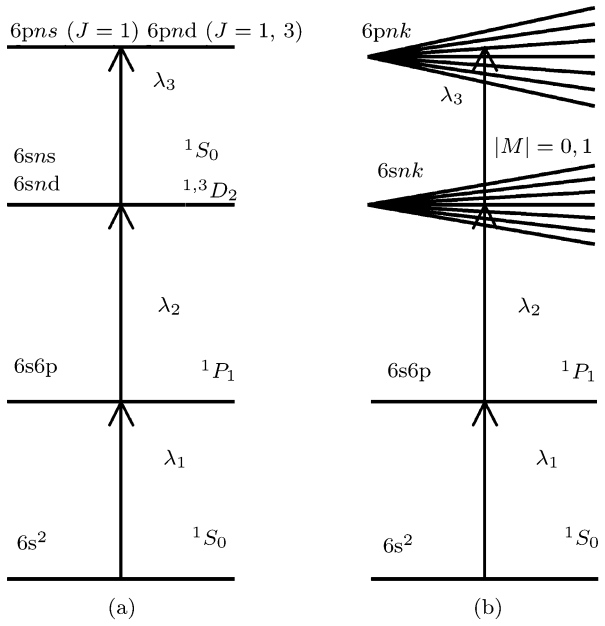


Fig.1. Three-step laser excitation scheme used in the experiment. (a) The first two lasers excite Ba atom to a desired 6sns $^1S_0$ or 6snd $^{1,3}D_2$ Rydberg states in zero field. The third laser is scanned to excite the core to the 6p state across the resonance line, resulting in the 6pns ($J = 1$) or 6pnd ($J = 1, 3$) autoionizing states in zero field. (b) The first two lasers excite Ba atom to the 6snk Stark states in electric fields, while the third laser is scanned to excite the 6pnk autoionizing states in electric fields.

Unlike the ICE case where the power density of the third laser is always reduced to avoid saturation effect, in the saturation excitation case the power density of the third laser is deliberately increased many times in order to observe more clearly the saturation effect on the autoionization spectrum. Meanwhile, the wavelength scanning of the third laser covers a much wider spectral range than in the corresponding ICE spectrum so that in the saturation excitation case many n members of the corresponding series can be excited simultaneously. The satellite features of these saturation spectra may provide some important information, which will be discussed in detail as follows.

Some errors have been corrected in order to ensure our experimental accuracy. For example, a hollow cathode lamp is used to calibrate the laser wavelength. It is worthwhile to note that it is more difficult to measure the autoionization spectra in electric fields due to the drastic increase in the number of states. Therefore, the wavelength calibration of the second laser is very crucial to distinguishing the right Stark states. On the other hand, in order to avoid some confusion in identifying the k and n values during the experiment, it is very helpful to set the wavelength of the second laser by referring to a theoretical Ba 6snk Stark map.[17] Also, the non-linearity in wavelength scans, especially during the wavelength scans of the third laser in the saturation case, has been considered. Contrary to the saturation case, an effort to eliminate saturation effect has been made in the process of measuring the ICE spectra because the power density of the third laser is crucial to the measurement of width for of an autoionizing state.[14]

3. Theoretical basis

The multi-channel quantum defect theory (MQDT) is regarded as a powerful tool, perhaps the best tool to interpret the ICE spectrum. In MQDT, the channel or Rydberg series is an important concept that is characterized by the corresponding quantum defect δ. Some relatively simple MQDT models have been adopted in the pioneer works, in which the MQDT parameters are obtained by the fitting procedure from the experimental data.[6,7,9] Up to now, with the help of R-matrix calculation, the MQDT has successfully reproduced the experimental spectra of Ba 6pnl autoionizing state in zero field.[7,11,18]

Here, we adopt the simplified MQDT formula in order to interpret the saturation effect more clearly. In zero field the Ba 6pnl autoionization spectra can be written in a closed form[4,19]

$$\sigma = \langle 6\mathrm{s}|D|6\mathrm{p}\rangle^2 O^2(v_\mathrm{i} v_\mathrm{f}) A_\mathrm{f}^2(v_\mathrm{f}). \qquad (1)$$

Here, $\langle 6\mathrm{s}|D|6\mathrm{p}\rangle$ is the dipole transition matrix of the core electrons determined by the states of core electrons. $A_\mathrm{f}(v_\mathrm{f})$, the spectral density, is a periodic function of the effective quantum of the final autoionizing states v_f. Usually, the spectral density is characterized by a regular series of Rydberg resonance, which may be far more difficult to calculate even with the help of R-matrix calculation.

$O(v_\mathrm{i} v_\mathrm{f})$ is the overlap integral that is determined by the overlap density between the initial bound 6snl

Rydberg state and the final 6pnl autoionizing state. The overlap integral can be expressed approximately as

$$O(v_\mathrm{i} v_\mathrm{f}) \propto \frac{\sin[\pi(v_\mathrm{f} - v_\mathrm{i})]}{E_\mathrm{f} - E_\mathrm{i}}, \tag{2}$$

where the initial and final Rydberg binding energies are $E_\mathrm{i} = 1/2v_\mathrm{i}^2$ and $E_\mathrm{f} = 1/2v_\mathrm{f}^2$ (in atomic units), respectively. When the wavefunction of initial bound Rydberg state is similar to the final autoionizing state, namely they have an equal effective quantum number or the difference between their effective quantum numbers is the integral, the zero of overlap integral is in superposition on the spectral density. Thus, the simple profile will appear in the spectrum according to the above formula. When the initial state wavefunction is obviously different from the final state wavefunction, there is no superposition for the zero in their wavefunctions. Therefore, the satellitic peaks will appear in their spectra under this condition. But, compared with the main transition in the ICE process, these peaks are so weak that they can be neglected in the spectrum.

Generally speaking, the ion signal I detected with MCP is determined by the optical cross section σ, the number of atoms in the bound Rydberg state I_0 and the integrated laser flux ϕ that is determined by the third laser power density. Specifically, the detected signals can be expressed as

$$I = I_0(1 - \mathrm{e}^{-\sigma\phi}). \tag{3}$$

From this equation, it is clear that the maximum signal is I_0. In the process of ICE, namely for the low laser density of the third laser, $\sigma\phi \ll 1$ is satisfied. Thus, the signal is proportional to the optical cross section and the integrated laser flux of the third laser, i.e. $I = I_0\sigma\phi$. However, when the laser power density is increased, the limit $\sigma\phi \ll 1$ will not hold any more, the increase of signal strength is not proportional to the laser power density, resulting in the appearance of satellitic peaks. In other words, the saturation effect occurs under the condition of high laser power density. The above equations will be used to discuss the saturation effect on the autoionization spectra in zero and electric fields.

Although the MQDT has been used successfully to interpret the saturation spectra of autoionizing states in zero field,[4,18,19] the electric field case is more complicated than the zero field case because the electric field effect adds complexity to the wave function. In an electric field, the quantum number l is no longer a good quantum number, a new quantum number k relevant to parabolic coordinates, has been introduced to describe the Stark states. Robicheaux[20] and Warntjes *et al*[21] extended the MQDT to the electric case and reproduced accurately the Mg 3pnk autoionization Stark spectra. However, it generally fails to reproduce the Ba 6pnk saturation spectra, probably due to the larger core of Ba atom and lack of spectral data in electric fields.[16] Thus, this experimental work about the Ba 6pnk saturation spectra in electric fields may enrich the experimental database and stimulate the theoretical studies in the future.

4. Results and discussion

4.1. The saturation spectra of 6pns ($J = 1$) autoionizing states

As mentioned above, one of the primary objectives of this work is to discuss the channel interaction by using the saturation spectrum. In order to observe the saturation effect on the 6pns ($J = 1$) autoionizing states the corresponding ICE spectra should be measured at first. A typical example of ICE spectrum with its saturation spectrum is shown in Fig.2.

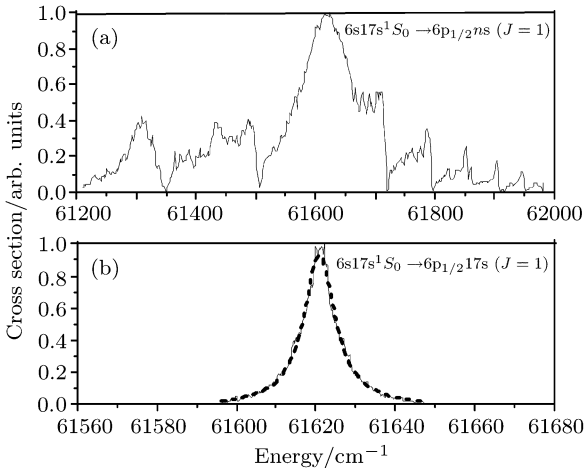


Fig.2. The spectra of 6p$_{1/2}n$s ($J = 1$) autoionizing states obtained in the experiment. (a) The saturation spectrum of 6p$_{1/2}$17s ($J = 1$) autoionizing state. (b) The ICE spectrum of 6p$_{1/2}$17s ($J = 1$) autoionizing state. The dotted curve represents the result from Lorentzian profile fitting.

The dotted curve in Fig.2(b) represents the Lorentzian profile fitting result, indicating that the 6p$_{1/2}$17s ($J = 1$) autoionization spectrum has the Lorentzian profile. In fact, the 6p$_{1/2}n$s ($J = 1$) and

$6p_{3/2}ns$ ($J = 1$) autoionization spectra other than the low n $6p_{3/2}ns$ ($J = 1$) spectra have the Lorentzian profiles due to the ICE method.[6,8] In the ICE process, because the first two lasers excite one valence electron to the Rydberg state far away from the core (so-called isolated core), in the third excitation step of the other valence electron the Rydberg electron can be avoided for unexpected perturbation. Thus, the experimental spectrum exhibits the Lorentzian profile, from which the level energies and widths can be extracted easily. For example, the level energy and width of the $6p_{1/2}17s$ ($J = 1$) autoionizing state can be determined from Fig.2(b) to be 61621.00 cm^{-1} and 9.62 cm^{-1}, respectively.

However, when the power density of the third laser is increased about 50 times greater than that in the ICE case and the wavelength of the third laser is scanned from the spectral position of 480 nm to 500 nm, the saturation spectrum of the $6p_{1/2}17s$ ($J = 1$) autoionizing state can be obtained as shown in Fig.2(a). In the figure the saturation effect emerges clearly in the $6p_{1/2}17s$ ($J = 1$) autoionization spectrum, in which many other $6p_{1/2}ns$ ($J = 1$) states are excited simultaneously. Under the condition of high laser power density, the linear relationship between the signal strength and laser power density no longer exists according to Eq.(3). Therefore, the saturation effect appears in the $6p_{1/2}17s$ ($J = 1$) autoionization spectrum, resulting in many satellitic peaks. Furthermore, with the knowledge of the effective quantum number of the 6s17s $^1S_0$ and $6p_{1/2}17s$ ($J = 1$) states, we conclude that their wavefunctions are different obviously from each other. Namely, the more sharp changes appearing on the right sides of the satellitic profiles (called blue shapes) indicate that the quantum defects of these $6p_{1/2}ns$ ($J = 1$) states are greater than that of the 6s17s $^1S_0$ Rydberg state. Also, it can be seen from the figure that several weaker peaks appear in the satellite profiles. This is due to the simultaneous excitation of the other 6pnd ($J = 1$) states in the saturation excitation process of $6p_{1/2}ns$ ($J = 1$) states because of the mixing of the 6pnl autoionizing states. In other words, the example shows that the excitation of the $6p_{1/2}$ core electron results in a complicated channel mixing in the third step.

But this is not the case for the $6p_{3/2}$ core state. An example of such saturation spectra, the saturation spectrum of the $6p_{3/2}26s$ ($J = 1$) autoionizing states, is shown in Fig.3(a).

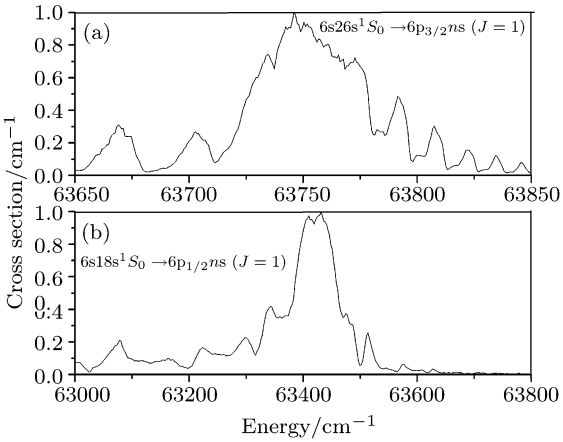


Fig.3. The saturation spectra of $6p_{3/2}ns$ ($J = 1$) autoionizing states obtained in the experiment. (a) Excited from the 6s26s $^1S_0$ state. (b) Excited from the 6s18s $^1S_0$ state.

This saturation spectrum can be observed under the condition similar to that of the $6p_{1/2}$ core case. It is clear that the satellite peaks almost exhibit the Lorentzian profile. The nearly symmetrical profile of the satellitic peak indicates that the effective quantum of the $6p_{3/2}ns$ ($J = 1$) autoionizing state is nearly equal to that of the 6s26s $^1S_0$ initial Rydberg state. For more careful check, it is obvious that many weaker peaks disappear in the satellitic profile, which is much different from the $6p_{1/2}ns$ ($J = 1$) saturation spectra. Another example, the saturation effect on the $6p_{3/2}18s$ ($J = 1$) autoionization spectrum, also confirms that the $6p_{3/2}ns$ ($J = 1$) saturation spectra have more simple satellitic profiles than those of the $6p_{1/2}ns$ ($J = 1$) saturation spectra. By checking all the $6p_{3/2}ns$ ($J = 1$) saturation spectra, we can conclude that besides the lower n members the $6p_{3/2}ns$ ($J = 1$) series is nearly an isolated series because it is not mixed with the other series.[4] The saturation spectrum not only can be used to analyse the channel mixing between the autoionizing series, but also has a particular application of determining the high n members or weak members of the autoionizing series. Figure 4 shows such two typical examples, the saturation spectra of the $6p_{1/2}24s$ ($J = 1$) and $6p_{3/2}33s$ ($J = 1$) states. In order to record these two saturation spectra, the power density of the third laser is increased about 100 times higher than that of their corresponding ICE case. Meanwhile, the third laser is scanned across a much broader spectral range for getting more n members. The energies of these members are listed in Table 1, in which the previous results obtained using the ICE method are also listed

for handy comparison.[4,18] Furthermore, the quantum defect δ can be deduced from the corresponding energy of autoionizing state E, namely $\delta = n - \sqrt{\frac{1}{2E}}$, which is also listed in Table 1. The quantum defect represents the difference between the main quantum number and effective quantum number, and reflects the interaction inside the atom system, such as the correlation between the valence electron and the core. From the table, one can see that the data from the saturation spectra are in agreement with the ICE data. Unlike our previous work, in the saturation spectra the width of satellite peaks cannot be extracted for the possible saturation effect on these satellite states. As mentioned above, it is difficult to excite the high n member of the autoionizing series or the weak state in the ICE process due to its poor signal density. However, the saturation excitation method overcomes this difficulty. Thus, it is suggested that the saturation excitation method should be extended to other atoms.

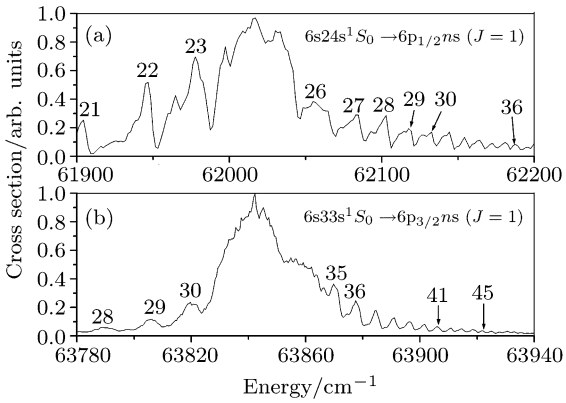


Fig.4. The saturation spectra of 6pns ($J = 1$) autoionizing states obtained in the experiment. (a) Excited from the 6s24s $^1S_0$ state to the 6p$_{3/2}ns$ ($J = 1$) autoionizing states. (b) Excited from the 6s33s $^1S_0$ state to the 6p$_{3/2}ns$ ($J = 1$) autoionizing states.

Table 1. Level energies and quantum defects of the high n members of Ba 6p$_{1/2}ns$ and 6p$_{3/2}ns$ ($J = 1$) autoionizing states. Uncertainty in the level energy E is about $\pm 0.30\,\mathrm{cm}^{-1}$.

6p$_{1/2}ns$	E/cm^{-1}		δ		6p$_{3/2}ns$	E/cm^{-1}		δ	
n	Pres.	[a]Prev.	Pres.	[a]Prev.	n	Pres.	[b]Prev.	Pres.	[b]Prev.
21	61902.10	61901.16	4.321	4.339	28	63793.08	63792.58	4.231	4.261
22	61943.75	61943.48	4.364	4.368	29	63807.24	63807.89	4.314	4.269
23	61982.02	61982.92	4.323	4.363	30	63821.13	63821.65	4.303	4.263
24	62014.84	62015.04	4.265	4.253	35	63871.73		4.188	
27	62084.42	62084.16	4.258	4.265	36	63878.42		4.255	
28	62101.23	62101.53	4.299	4.273	37	63884.76		4.289	
29	62116.44	62116.84	4.319	4.268	38	63890.60		4.316	
30	62130.31	62130.55	4.310	4.281	39	63896.18		4.300	
31	62142.69	62142.63	4.297	4.291	40	63901.26		4.291	
32	62153.45	62153.43	4.312	4.301	41	63905.57		4.361	
33	62163.54	62163.22	4.281	4.301	42	63909.87		4.358	
34	62172.27	62172.07	4.289	4.314	43	63913.85		4.352	
35	62180.21	62180.05	4.293	4.315					
36	62187.49	62187.27	4.285	4.318					

a. The data from Ref.[10]

b. The data from Ref.[5]

4.2. The saturation spectra of 6pnd (J= 1, 3) autoionizing states

The spectra of 6pnd ($J = 1, 3$) autoionizing states are more complex than those of the 6pns ($J = 1$) autoionizing states mainly due to two factors. One is that the 6pnd ($J = 1, 3$) autoionizing state always includes two components, the 6pnd ($J = 1$) and 6pnd ($J = 3$) states. The other is that the 6pnd ($J = 1, 3$) autoionizing state involves more channels, which may interact with each other. Such an example is shown in Fig.5(a). It is clear from the figure that the spectrum of the 6p$_{3/2}$13d ($J = 1, 3$) autoionization state has a multi-peak structure. With the help of the multi-peak Lorentzian fitting, the four components, the 6p$_{3/2}$13d$_{3/2}$ ($J = 1$), the 6p$_{3/2}$13d$_{5/2}$ ($J = 1$), the 6p$_{3/2}$13d$_{3/2}$ ($J = 3$) and 6p$_{3/2}$13d$_{5/2}$ ($J = 3$) states, can be identified from the spectrum accurately. The detailed properties of the 6p$_{3/2}n$d ($J = 1, 3$) states reveal the channel interaction between the 6pnl au-

toionizing series, which have been discussed in our previous work.[9] However, the complex structure of the $6p_{3/2}nd$ ($J = 1, 3$) spectra results in an impossibility to observe their saturation effects because it is too complicated to determine the components excited in saturation spectrum. Contrary to the $6p_{3/2}nd$ ($J = 1, 3$) autoionization spectra, this is not the case for the $6p_{1/2}$ core. A typical example, the spectrum of $6p_{1/2}13d$ ($J = 1, 3$) state excited from the $6s13d\ ^1D_2$ state, is shown in Fig.5(b), which exhibits nearly a single Lorentzian profile. This fact indicates that the two components, the $6p_{1/2}13d$ ($J = 1$) and $6p_{3/2}13d$ ($J = 3$) states, cannot be distinguished under the experimental condition. More experimental results confirm further that almost all the $6p_{1/2}nd$ ($J = 1, 3$) states show mono-peak, which are similar to the $6p_{1/2}13d$ ($J = 1, 3$) states.

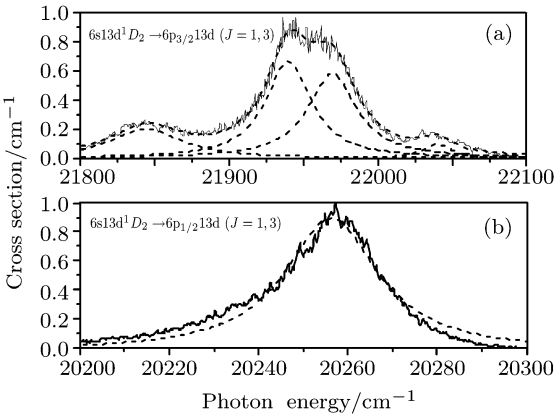


Fig.5. Typical ICE spectra of $6pnd$ ($J = 1, 3$) autoionizing states with Lorentzian-profile fittings. The full curves represent the experimental spectra, while the dotted curves are obtained from Lorentzian fitting. (a) The spectrum of the $6p_{3/2}13d$ ($J = 1, 3$) autoionizing states with multi-peak Lorentzian profile fitting. (b) The spectrum of the $6p_{1/2}13d$ ($J = 1, 3$) autoionizing states with mono-peak Lorentzian profile fitting.

Therefore, only the saturation spectra of the $6p_{1/2}nd$ ($J = 1, 3$) states are discussed in this paper. Two examples of the $6p_{1/2}nd$ ($J = 1, 3$) saturation spectra, the $6p_{1/2}29d$ ($J = 1, 3$) and $6p_{1/2}19d$ ($J = 1, 3$) autoionization spectra, are shown in Figs.6(a) and (b), respectively. The saturation spectrum of $6p_{1/2}29d$ ($J = 1, 3$) state is excited from the $6s29d\ ^1D_2$ state. This saturation spectrum is evidently similar to the $6p_{3/2}ns$ ($J = 1$) autoionizing states. But the satellites have more blue sharp profiles than those of $6p_{3/2}ns$ ($J = 1$) autoionizing states. This fact indicates that the differences of quantum defects between the $6p_{1/2}nd$ ($J = 1, 3$) states and the $6s29d\ ^1D_2$ state are greater than those between the $6p_{3/2}ns$ ($J = 1$) states and the $6s24s\ ^1S_0$ state. In order to record more satellites, the $6p_{1/2}19d$ ($J = 1, 3$) saturation spectrum with high saturation degree is shown in Fig.6(b), where many $6p_{1/2}nd$ ($J = 1, 3$) states can be defined in the saturation spectrum. Similar to the $6pns$ ($J = 1$) case, the level energies of these high n states are extracted from the saturation spectrum and are listed in Table 2. At the same time, the quantum defects of these high n states are deduced from their corresponding state energies also listed in the table. The present data agree with the previous data obtained from the ICE spectra, which is also listed in the table for comparison.[9]

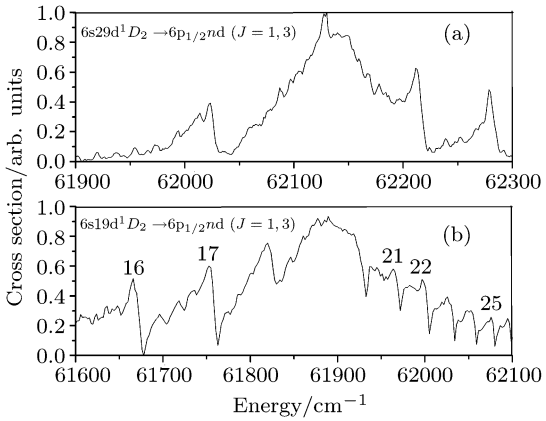


Fig.6. The saturation spectra of $6p_{1/2}nd$ ($J = 1, 3$) autoionizing states obtained in the experiment. (a) Excited from the $6s29d\ ^1D_2$ state. (b) Excited from the $6s19d\ ^1D_2$ state.

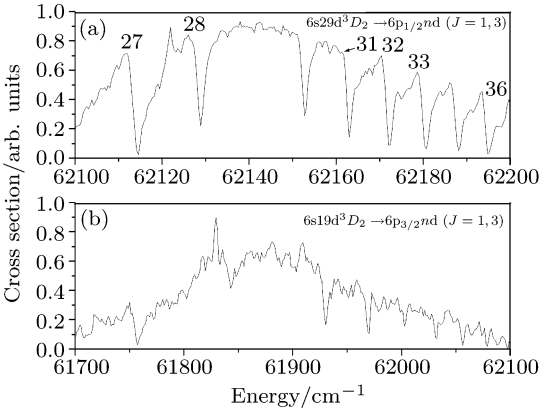


Fig.7. The saturation spectra of $6p_{1/2}nd$ ($J = 1, 3$) autoionizing states obtained in the experiment. (a) Excited from the $6s29d\ ^3D_2$ state. (b) Excited from the $6s19d\ ^3D_2$ state.

It is well known that the initial $6snd$ Rydberg states have two series, the $6snd\ ^1D_2$ and $6snd\ ^3D_2$

series due to the orbit-spin coupling of Rydberg electrons. Thus, the final $6p_{1/2}nd$ (J = 1, 3) states are more complex than the 6pns (J = 1) states. To explore such a complex structure, the saturation spectra of the $6p_{1/2}nd$ (J = 1, 3) states excited from the 6snd $^3D_2$ Rydberg states are also measured in the experiment. Two examples are shown in Fig.7, which are excited from the 6s29d $^3D_2$ and 6s19d $^3D_2$ Rydberg states, respectively. The figure confirms that the saturation spectra of the $6p_{1/2}nd$ states are more complex than those from the singlet states. Especially, compared with the $6p_{1/2}19d$ (J = 1, 3) spectrum shown in Fig.6(b), the $6p_{1/2}19d$ (J = 1, 3) spectrum excited from 6s19d $^3D_2$ Rydberg states has obviously complex structures of its profile, which is probably due to the more complicated channel mixing. However, the $6p_{1/2}29d$ (J = 1, 3) saturation spectrum is not the case as shown in Fig.7(a), from which the level energies of the high n $6p_{1/2}nd$ (J = 1, 3) states can be determined and are in good agreement with the previous data listed in Table 2.

Table 2. Level energies and quantum defects of the high n members of Ba $6p_{1/2}nd$ (J = 1, 3) autoionizing states excited from the 6snd $^1D_2$ and 6snd $^1D_2$ states, separately. Uncertainty in the level energy E is about ± 0.30 cm^{-1}.

$6p_{1/2}nd$	E/cm^{-1}		δ		$6p_{3/2}nd$	n	E/cm^{-1}	δ	
n	Pres.	[a]Prev.	Pres.	Prev.	n	Pres.	[b]Prev.	Pres.	Prev.
[c]16	61676.83	61677.80	2.693	2.683	[d]27	62106.12		2.997	
17	61757.82	61758.27	2.728	2.350	28	62121.21		2.985	
18	61823.96	61823.56	2.762	2.769	31	62157.15		2.946	
21	61964.52	61964.91	2.821	2.810	32	62167.07		2.892	
22	62004.73	62004.97	2.609	2.602	33	62174.05		3.074	
23	62031.32	62031.18	2.660	2.667	34	62182.82		2.942	
24	62054.74	62054.54	2.698	2.708	35	62190.43		2.848	
25	62075.35	62075.11	2.729	2.741	36	62196.82		2.835	

a. Data from Ref.[11]
b. No data available.
c. The $6p_{1/2}nd$ (J = 1, 3) states excited from the 6snd $^1D_2$ Rydberg states.
d. The $6p_{1/2}nd$ (J = 1, 3) states excited from the 6snd $^3D_2$ Rydberg states.

4.3. The saturation spectra of 6pnk ($|M| = 0, 1$) autoionizing Stark states

Similar to the zero field case, it is necessary to record the ICE spectrum in order to obtain the saturation spectrum in electric field. These individual ICE spectra in electric field represent the corresponding autoionizing Stark states, which are different from those of scaled-energy spectroscopy ($|M| = 0, 1$) in electric field.[22,23] The example of such a saturation spectrum accompanying with its ICE spectrum is shown in Fig.8. The saturation spectrum of $6p_{3/2}13k$ states with $M = 0, k = 2$ at $F = 3500$ V/cm is shown in Fig.8(a) while the ICE spectrum is shown in Fig.8(b). From the figure, it is clear that the 6pnk autoionization spectrum has simple symmetric profiles, where the dotted curve is the result from the Lorentzian profile fitting. This fact is similar to the zero field case where the autoionization spectrum has the Lorentzian profile. This result indicates that the effect of electric field on the transition of the third step can be neglected in the excitation process, which has been described in our previous work.[12] In order to record its saturation spectrum, the power density of the third laser is increased about 20 times higher than that for the ICE spectrum. Figure 8(a) shows such a saturation effect on the autoionizing Stark states. Many satellite features appearing in the spectrum indicate that the nk Rydberg Stark electrons are perturbed by the third step transition in the electric fields, which is similar to the zero field case. Surprisingly, many weak peaks appear in the main profile of the saturation spectrum. We check this spectrum many times and can conclude that these peaks presumably originate from the state mixing in the presence of electric field.

More examples with different core states and electric field strengths are shown in Fig.9. The figure shows the saturation spectrum of $6p_{1/2}14k$ states

with $|M| = 1, k = 1$ at $F = 5000\,\mathrm{V/cm}$ and that of $6p_{3/2}14k$ states with $|M| = 1, k = 1$ at $F = 2500\,\mathrm{V/cm}$. Comparing between these two spectra, one may conclude that it is harder to excite the saturation spectrum of the $6p_{1/2}14k$ states, because the transition 6s to $6p_{3/2}$ states is weaker than to the $6p_{1/2}$ states. Therefore, the saturation effect on the $6p_{1/2}14k$ spectrum is more obvious than on $6p_{3/2}14k$ spectrum under the same experimental condition. Furthermore, by careful check it is clear that they all have symmetric profiles, which is similar to the zero field case mentioned above. This fact further confirms that the electric field cannot affect the core electron transition.

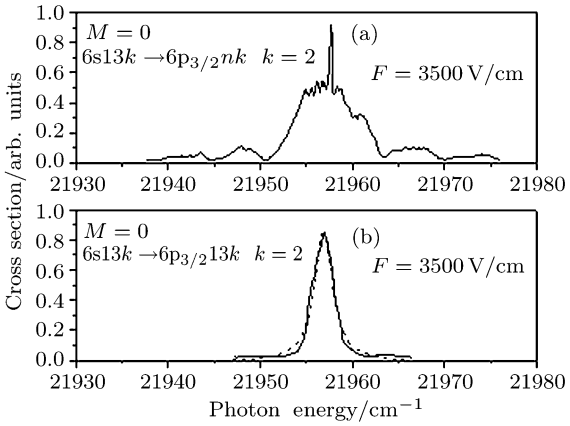


Fig.8. Typical ICE and saturation spectrum of the 6pnk autoionizing Stark states. (a) The saturation spectrum of the $6p_{1/2}13k$ autoionizing state with $M = 0, k = 2$ and $F = 3500\,\mathrm{V/cm}$. (b) The ICE spectrum of the $6p_{1/2}13k$ autoionizing state with $M = 0, k = 2$ and $F = 3500\,\mathrm{V/cm}$. The dotted curve is from the Lorentzian profile fitting.

In order to explore the dependence of an autoionization saturation spectrum on the electric field, the saturation spectra of the $6p_{3/2}15k$ states with $|M| = 0$, $k = 4$ are measured at the different strengths of electric field $F = 2000, 2500$, and $3000\,\mathrm{V/cm}$ as shown in Fig.10. These curves indicate that the structures in the saturation spectra of the autoionizing Stark states have little changes with the strength of the electric field. The satellitic profiles appearing in the main profile is very similar to those observed in the ICE spectrum.[14] In the ICE process, the electric field can affect the Rydberg electron wavefunction, and thereby lead to the un-superposition of the core and Rydberg electron wave functions. However, it is necessary to point out that these similar peaks are very different in their origination mechanisms. Primarily, the experimental conditions are different for these two types of peaks. The satellitic peaks in the ICE spectrum are from the ICE process while the satellitic peaks in saturation spectrum are obtained under the saturation condition. Concretely, the autoionizing state mixing leads to the satellitic profiles in the ICE spectrum, while the satellitic peaks in saturation spectrum are from the saturation effect on the autoionization spectrum. Furthermore, by detailed comparison one can know that the structure of autoionization Stark spectrum varies with the electric field as shown in Fig.10. But, this is not the case for the saturation excitation. So far, there has been not an appropriate theory to interpret the saturation spectrum in the electric field. These observations may stimulate corresponding theoretical works in the future.

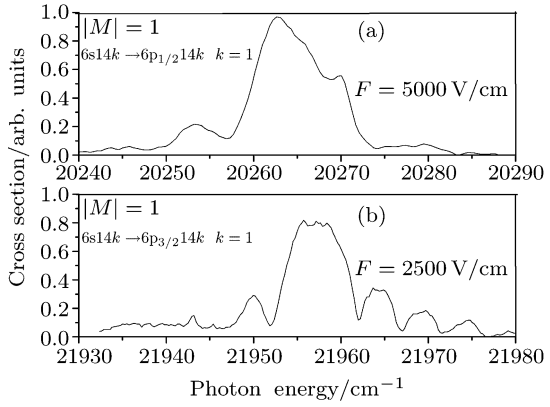


Fig.9. The saturation spectra of the 6pnk autoionizing Stark states. (a) The saturation spectrum of the $6p_{1/2}14k$ autoionizing state with $|M| = 1, k = 1$ and $F = 5000\,\mathrm{V/cm}$. (b) The saturation spectrum of the $6p_{3/2}14k$ autoionizing state with $|M| = 1, k = 1$ and $F = 2500\,\mathrm{V/cm}$.

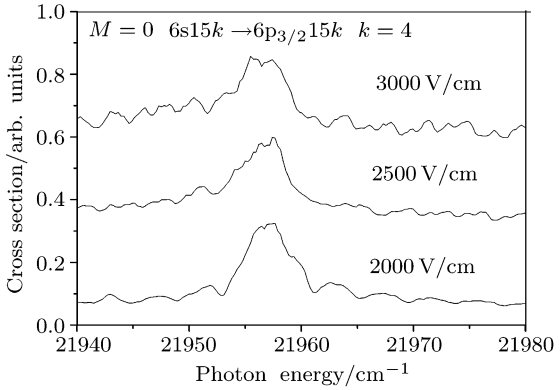


Fig.10. The saturation spectra of the $6p_{3/2}15k$ autoionizing state with $|M| = 0$ and $k = 4$ for $F = 2000$, 2500 and $3000\,\mathrm{V/cm}$.

5. Conclusion

In this paper, the three-step laser excitation technique has been used to measure the saturation autoionizing spectra in zero and electric fields, separately. Combined with the proper laser polarization, we have applied this method to the study of Ba atom, where the saturation spectra of the 6pnl (l = 0, 2) autoionizing states and the 6pnk ($|M|$ = 0, 1) Stark states have been measured and analysed in detail for cases of both zero and electric fields. Experimental results show that the saturation spectrum is an efficient method to determine the high n members of the autoionizing series and discuss the channel interactions in zero field. On the other hand, the saturation spectra in electric fields show that the satellitic profiles originate from the electric field effect, which can help us to understand more of the behaviours of the autoionizing states in the electric field.

References

[1] Dai C J, Schinn G W and Gallagher T F 1990 *Phys. Rev.* A **42** 223

[2] Xu E Y, Zhu Y F, Mullins O C and Gallagher T F 1986 *Phys. Rev.* A **33** 2401

[3] Dai C J 1994 *Acta Phys. Sin.* **43** 369 (in Chinese)

[4] Kachru R, van Linden van den Heuvell H B and Gallagher T F 1985 *Phys. Rev.* A **31** 700

[5] Li S B, Dai C J, Sun W and Xue P 2001 *J. Phys.* B **34** 2123

[6] Bhatti S A, Cromer C L, Cooke W E 1981 *Phys. Rev.* A **24** 161

[7] Cooke W E, Bhatti S A and Cromer C L 1982 *Opt. Lett* **7** 69

[8] Eichmann U, Lange V and Sandner W 1991 *Phys. Rev. Lett.* **68** 21

[9] Mullins O C, Zhu Y F, Xu E Y and Gallagher T F 1985 *Phys. Rev.* A **32** 2234

[10] Li S B, Dai C J and Zhang Y 2002 *Chin. Phys.* **11** 690

[11] Zhang Y, Dai C J and Li S B 2004 *J. Electron Spectrosc. Relat. Phenom.* **135** 63

[12] Li S B and Dai C J 2004 *J. Electron Spectrosc. Relat. Phenom.* **136** 247

[13] Jones R R and Gallagher T F 1989 *Phys. Rev.* A **39** 4583

[14] Li S B and Dai C J 2003 *J. Electron Spectrosc. Relat. Phenom.* **130** 43

[15] Liu Y P, Dai C J and Li S B 2004 *J. Electron Spectrosc. Relat. Phenom.* **142** 91

[16] Jones R R, Lyons B J, Baig M A, Djambova S T and Gallagher T F 2000 *Phys. Rev.* A **62** 033408

[17] Zhi M C, Dai C J and Li S B 2001 *Chin. Phys.* **10** 929

[18] Lange V, Aymar M, Elchmann U, Sandner W 1991 *J. Phys.* B **24** 91

[19] Kachru R, Tran N H, Pillet P and Gallagher T F 1985 *Phys. Rev.* A **31** 218

[20] Robicheaux F 2000 *Phys. Rev.* A **62** 033406

[21] Warntjes J B M, Robicheaux F and Noordam L D 2000 *Phys. Rev.* A **62** 033407

[22] Ni N, Cao J W, Wang C and Zhan M S 2004 *Acta Phys. Sin.* **53** 1335 (in Chinese)

[23] Liu X J, Cao J W, Wang J, Zhao H T and Zhan M S 2000 *Acta Phys. Sin.* **49** 1447 (in Chinese)